where $\theta = 2\pi f$ and $X_{c\,M\text{-}PDC}$ is the continuous part of the PSD. Note that since the code is DC balanced in all the positions, this is the expected value $E\{a_n\} = 0$, discrete spectral lines are absent [3]. This PSD is normalised to the bit rate, and the spectrums are not in a range of 0 to 1, as the PSDs are normally shown. This normalisation is made so that we can see how the spectrum changes with respect to M.

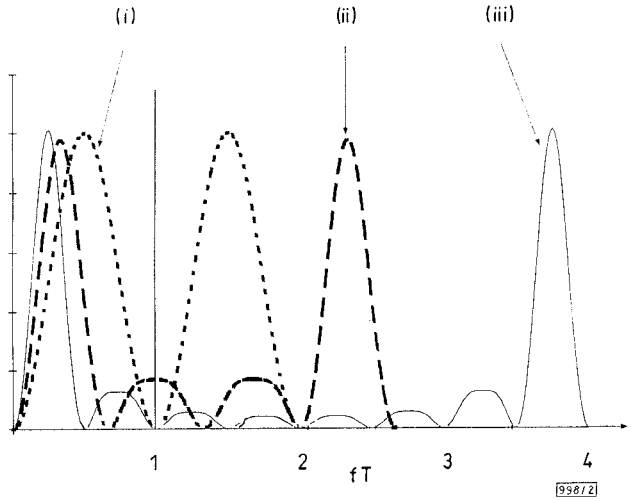

Fig. 2 *Normalised power spectral density of M-PDC*

(i) 2-PDC
(ii) 3-PDC
(iii) 4-PDC

The graphics of the PSD are shown in Fig. 2. This Figure shows the relative bandwidth for the presented codes. The numbers in the horizontal axis are the product of fT.

Conclusions: We have analysed, in a general manner, the M-PDC coding scheme, taking the QP coding scheme as a basis and presenting the codewords for 3-PDC and 4-PDC. The word synchronisation at the receiver was also analysed. The M-PDC scheme has a feature that can detect errors in the symbols read. This is owing to the shape of the codeword, which must satisfy eqn. 1. We also have analytically obtained the PSD of 2-PDC, 3-PDC and 4-PDC, which had not been obtained before. From the PSD we can infer that this code family is suitable for DMR because it has a null of zero frequency and of a symbol rate of $1/\tau$. This code family is also limited in a run length of 0's and 1's, due to the block coding, and each codeword has at least one zero-crossing every M bit periods, which means that we can obtain a good clock signal for receiver synchronisation.

20 January 1997

Electronics Letters Online No: 19970384

D. Muñoz-Rodríguez and F. de J. Ambríz-Hernández (*Instituto Tecnologico y Estudios Superiores de Monterrey, Centro de Electronica y Telecomunicaciones, Suc. de Correos 'J', Monterrey, N.L. C.P 64849, Mexico*)

References

1 BERGMANS, J.W.M.: 'Two new equalisation schemes for high density digital magnetic recording systems with quad-phase modulation code', *Electron. Lett.*, 1990, pp. 13–15

2 BERGMANS, J.W.M.: 'Baud-rate data-aided timing recovery for digital magnetic recording systems with quadra-phase modulation code', *IEEE Trans. Commun.*, 1995, pp. 2012–2015

3 CARIOLARO, G.L., and TRONCA, G.P.: 'Spectra of block coded digital signals', *IEEE Trans. Commun.*, 1974, pp. 1555–1564

4 BIXBY, J.A., and KETCHAM, R.A.: 'Q.P., an improved code for high density digital recording', *IEEE Trans. Magn.*, 1979, pp. 1465–1467

5 CATTERMOLE, K.W., and O'REILLY, J.J.: 'Mathematical topics in telecommunications, vol. 2'. 'Problems of randomness in communication engineering' (Pentech Press, 1984), chap. 15, pp. 272–300

MOS magnetic current sensor based on standard CMOS process

Hong-Ming Yang, Tan-Fu Lei, Yu-Chung Huang and Chung-Len Lee

Indexing term: Magnetic sensors

A novel current sensor is proposed. The current sensor consists of one MOS magnetic sensor and a flat coil in an industrial CMOS process. An experimental device demonstrated a sensitivity of 8.4mV/A.

Recently, research was dedicated to developing solid state microsensors based on the CMOS process [1 – 5] for the detection of magnetic fields. For example, Gallagher and Corak [3] proposed an MOS magnetic field sensor with rectangular regions consisting of two Hall probes placed symmetrically across the channel to detect the magnetic field. In another example, Andrä *et al.* [4] developed a current sensor using a magnetoresistive material on an insulating multilayer to detect current.

In this Letter, we report a new current sensor based on standard CMOS processing. The sensor has a high sensitivity owing to its current coil, fabricated on the second metal layer, being very close to the magnetic sensing MOS device underneath. In addition, it has a better linearity than the magnetoresitive type of sensor since the magnetic sensing MOS device has a better linearity.

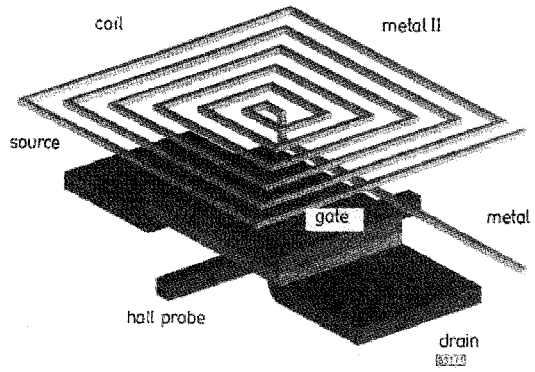

Fig. 1 *Current sensor consisting of one coil and one MOS magnetic sensor*

The device is shown in Fig. 1, where the current coil is made of the second metal of the standard single-poly-double-metal CMOS process and the magnetic sensing MOS is an N-type MOS transistor underneath which a pair of Hall probes [5] are located laterally. When current flows through the coil, it creates a magnetic field which is detected by the MOS Hall magnetic sensing device underneath. This current sensor can be readily integrated with other standard CMOS circuits without any additonal processing steps.

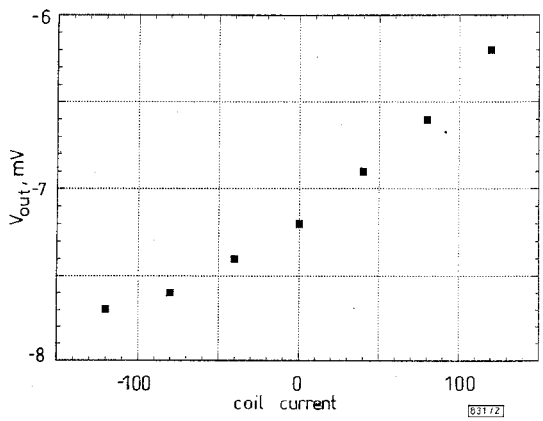

Fig. 2 *Current sensor output against measured current*

An experimental version of the above sensor was fabricated so that its characteristics could be measured. For this device, the MOS transistor had a W/L = 30μm/25μm and the Hall probes

were located at $y/L = 0.7$ [5] and its sensitivity was 90mV/Tesla when it operated at $Vg = Vd = 5$V. The coil was designed with a 10μm line width, 2.5μm line spacing of Al metal layer and the total area was $(400\mu m)^2$. Fig. 2 shows the measured DC Hall voltage of the MOS magnetic sensor against coil current. It is seen that the Hall voltage is nearly linear with respect to the coil current. The sensitivity of the current sensor was ~8.4mV/A. When the current flowed in the opposite direction, the Hall voltage also decreased. The device had a offset Hall voltage when the input coil current was zero. This might result from the misalignment of the Hall probes, the piezoresistance effect, or the mechanical stress in the package. However, it can be compensated for during the readout circuit design when it is to be integrated into a CMOS circuit.

In conclusion, this Letter reports and demonstrates a novel current sensor, which is compatible with the conventional CMOS process. It has a linear and high sensitivity. An experimental device exhibited a sensitivity of 8.4mV/A.

Acknowledgments: The authors would like to thank W.-H. Ko for his suggestion, the co-workers of CIC for their device design and S.-C. Chao for his help.

6 January 1997
Electronics Letters Online No: 19970375

Hong-Ming Yang, Tan-Fu Lei, Yu-Chung Huang and Chung-Len Lee (*Department of Electronics Engineering and Institute of Electronics, National Chiao Tung University, Hsinchu, Taiwan, Republic of China*)

E-mail: U8111805@cc.nctu.edu.tw

References

1 SMY, T., and RISTIC, LJ.: 'Optimization of magnetotransistor structure in CMOS technology', *IEEE Trans.*, 1992, **MAG-28**, (5), pp. 2024–2030
2 PARANJAPE, M., FILANOVSKY, I., and RISTIC, LJ.: 'A 3-D vertical Hall magnetic-field sensor in CMOS technology', *Sens. Actuators A*, 1992, **34**, pp. 9–14
3 GALLAGHER, R.C., and CORAK, W.S.: 'A metal-oxide-semiconductor (MOS) Hall element', *Solid-State Electron.*, 1966, **9**, pp. 571–580
4 ANDRÄ, W., KÜHNAND, S., and PERTSCH, P.: 'Current measurements based on thin-film magnetoresistive sensors', *Sens. Actuators A*, 1993, **37–38**, pp. 461–465
5 MATHIEU, N., GIORDANO, P., and CHOVET, A.: 'Si MAGFETs optimized for sensitivity and noise properties', *Sens. Actuators A*, 1992, **32**, pp. 656–660

10Gbit/s, 10600km, dispersion-allocated soliton transmission using conventional 1.3μm singlemode fibres

E. Yamada, H. Kubota, T. Yamamoto, A. Sahara and M. Nakazawa

Indexing terms: Soliton transmission, Optical communication

A 10Gbit/s data signal at 1.55μm has been successfully transmitted over 10600km using a dispersion-allocated soliton technique and 1.3μm singlemode fibres.

The dispersion-allocated soliton technique [1] allows us to utilise optical fibres with various dispersions as soliton transmission fibres. This technique uses fibres with large normal and anomalous group velocity dispersions which are obtained by keeping the average GVD small and anomalous. Therefore, when the soliton pulse, which is determined by the average GVD, is coupled into a fibre, it behaves like a linear pulse. In other words, we can increase the transmitted power because the GVD in each segment is much larger than the average value. Therefore, we can obtain a dispersion-allocated soliton with a better signal to noise ratio by launching a pulse with a higher power than that required for a conventional soliton transmission [2, 3]. When we increase the pulse power with the conventional soliton technique, the pulse waveform and its spectrum change as the high order soliton is excited. However, there is no such disadvantage with the dispersion-allocated soliton.

It is also important to note that the Gordon-Haus jitter can be reduced by adopting a small average dispersion [4]. When the dispersion allocation is small, or the allocation distance is short, the system can be well described with a perturbed nonlinear Schrödinger equation and a stable sech-shaped soliton pulse can be transmitted. When the dispersion allocation is large, the transmitted pulse changes from an ideal sech pulse to a Gaussian pulse, but it is still stable as the soliton effect is partly incorporated. In addition, it is also important to note that four-wave mixing is less excited when the average GVD is not zero. Therefore, when the average GVD is set at zero as in the conventional technique, four-wave mixing is excited considerably since phase matching is easily achieved at zero dispersion.

Of particular benefit is the fact that it allows the practical realisation of a soliton transmission system [5]. Specifically, if this technique can be applied with conventional fibre, the enormous stock of 1.3μm singlemode fibre which has already been installed will have new value as a high capacity transmission line. To this end, a large number of NRZ transmission experiments with dispersion compensation have been undertaken, however, only a few experiments have been performed on soliton data transmission [6]. Knox *et al.* showed that a transmission of 10Gbit/s over 2020km was possible with an amplifier spacing of 33km [7]. We have numerically confirmed that a D-A soliton signal is superior to an NRZ signal or an Rz pulse at zero GVD for this purpose [8].

Here, we demonstrate experimentally for the first time, a 10Gbit/s 10600km dispersion-allocated soliton data transmission at 1.55μm using conventional 1.3μm optical fibres.

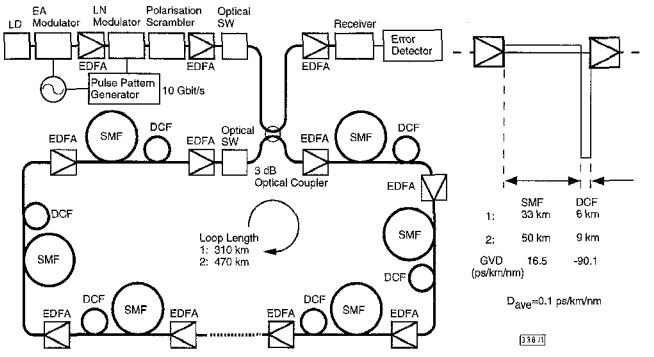

Fig. 1 *Experimental setup using 1.3μm SMF*

Fig. 1 shows the experimental setup for a 10Gbit/s data transmission using 1.3μm singlemode fibres (SMF) and dispersion compensation fibres (DCF). We prepared two configurations. In one configuration, the amplifier spacing was 39km, where a 33km SMF was succeeded by a 6km DCF, and the loop length was 312km. In the other configuration, the amplifier spacing was 59km, where a 50km SMF was succeeded by a 9km DCF, and the loop length was 472km. The average group velocity dispersion was 0.1ps/km/nm. The pulsewidth was 16ps, the signal wavelength was 1.553μm, and the data length was 2^7–1 PRBS. The fibre loop consisted of eight amplifier spans, with eight 0.98μm pumped erbium-doped fibre amplifiers (EDFAs) and one 1.48μm pumped EDFA. In the first configuration, the input optical power was 3dBm. We incorporated a slow speed polarisation scrambler to eliminate the polarisation hole burning effect in the EDFAs.

Bit error rate (BER) curves before and after the 10000km transmission are shown in Fig. 2. A BER below 10^{-9} was achieved with a received optical power of –27dBm. The power penalty at that point was 5.2dB. The inset photograph shows the eye diagram after a 10000km transmission, which indicates a clear eye opening.

Fig. 3 shows the BER obtained against transmission distance. A bit error rate of 10^{-9} was achieved at 10600km. This result agrees with our numerical simulation which gives a maximum transmission distance of >11000km. Even when the amplifier spacing was extended to 59km (50km SMF and 9km DCF), a BER below 10^{-9} was achieved at a transmission distance of 9200km. As there is no significant difference between these results, it can be said that the